JOURNAL OF AGRICULTURAL AND FOOD CHEMISTRY

ARTICLE

pubs.acs.org/JAFC

# Biosynthesis of Methoxypyrazines: Elucidating the Structural/Functional Relationship of Two *Vitis vinifera O*-Methyltransferases Capable of Catalyzing the Putative Final Step of the Biosynthesis of 3-Alkyl-2-Methoxypyrazine.

José G. Vallarino,[†,⊥] Xaviera A. López-Cortés,[‡,⊥] Jake D. Dunlevy,[§,∥] Paul K. Boss,[∥] Fernando D. González-Nilo,[‡] and Yerko M. Moreno[†,*]

[†]Centro Tecnológico de la Vid y el Vino, Facultad de Ciencias Agrarias, Universidad de Talca, Chile

[‡]Centro de Bioinformática y Simulación Molecular, Universidad de Talca, Chile

[§]School of Biological Sciences, Flinders University of South Australia, Australia.

[∥]CSIRO Plant Industry, Glen Osmond, Australia

**ABSTRACT:** 3-Alkyl-2-methoxypyrazines (MPs) are an important food constituent and have been associated with detrimental herbaceous flavors in red wines by consumers and the wine industry. The *Vitis vinifera* genes *O*-methyltransferase 1 and 2 (*VvOMT1* and *VvOMT2*) have been isolated in the grapevine cultivar Carmenere. These genes encode *S*-adenosyl-L-methionine (SAM)-dependent *O*-methyltransferases, which have the ability to methylate 3-alkyl-2-hydroxypyrazines (HPs)—the putative final step in MPs production. Atomic studies were performed in order to explain the differences in these VvOMT activities through their structural/functional relationship in MPs biosynthesis. Differences in enthalpy energy observed between the proteins may be due to changes of equivalent residues in the active sites of VvOMT1 (F319, L322) and VvOMT2 (L319, V322). However, docking simulations and QM/MM analyses described how residues H272 and M182 could explain the main functional differentiation observed between VvOMT1 and VvOMT2 through steric impediment, which limits the formation of the transition state in enzymes encoded by *VvOMT2*. Therefore, this finding could explain the decreasing catalytic efficiency observed for VvOMT2.

**KEYWORDS:** methoxypyrazines, methyltransferases, *Vitis vinifera*, wine, flavor, docking simulation, QM/MM

## INTRODUCTION

Nature is full of aromas and flavors, and they are directly linked to food and beverage preference and palatability. Pyrazines are compounds widely distributed in the plant and animal kingdoms and include some of the most potent odorants known, such as the 3-alkyl-2-methoxypyrazines (MPs), which have extremely low sensory detection thresholds as low as 2 ppt in water and 15 ppt in wine.[1] MPs are an important group of natural flavor constituents of some foods and raw vegetables [2−5] including grapes (*Vitis vinifera*).[6,7] In this regard, 3-isobutyl-2-methoxypyrazine (IBMP) and 3-isopropyl-2-methoxypyrazine (IPMP) have been found to play an important role in the detrimental herbaceous flavor of several red wine cultivars such as Cabernet Sauvignon, Merlot,[8] Cabernet Franc,[1] and Carmenere.[9] However, it also contributes to a more acceptable vegetative varietal aroma in white wine cultivars such as Sauvignon blanc, Chardonnay, Semillon, and Riesling.[10,11] The main aromatic descriptor associated with IBMP is described as a green pepper aroma, which provides unappealing features in Carmenere red wines. Furthermore, this cultivar produces the highest levels reported in the literature, and it is a recurrent aromatic attribute when describing these wines.[9]

The first report on the role of MPs in the flavor of grapes or wine was in 1975 concerning the Cabernet Sauvignon cultivar.[6] Many papers have since been published and report on MPs concentrations in different grapevine tissues, grape berries, and wines of different cultivars and the association of this compound with green or vegetal aromas.[1,3−10,12,13] Different factors can affect the presence of MPs in grapes and wines such as climate and soil, temperature, light, grape ripening, as well as viticultural and enological practices. Climatic conditions have a critical effect upon MPs concentration in grapes.[9] Vines planted in cool climates tend to contain higher levels of MPs,[14] but it is unclear whether this is due to higher MPs production or a lower degradation rate.[11]The role that light/temperature plays in the degradation of MPs is not fully understood.[11,15] It is known that MPs levels in grapevines decrease during grape ripening, and this occurs after veraison.[1,16] The MPs location and concentration in bunches and berries have also been determined.[7,8] It has been reported that field viticultural practices, such as irrigation regimes, planting density, and canopy modifications, can modify the MPs levels in grapes.[12,15,17,18] Enological practices during winemaking such as the amount of skin contact[19] and the presence of stem remnants during vinification also affect wine MPs concentrations.[20] There are also studies covering the effects of the lady beetle (*Harmonia axyridis*) or yeast strain (*Saccharomyces cerevisiae*) used in winemaking and their relation to MPs.[21,22] The accumulation and degradation curves of MPs in grapevines and how some factors can modify its concentration during the

**Received:** October 18, 2010
**Accepted:** May 18, 2011
**Revised:** May 16, 2011
**Published:** May 18, 2011

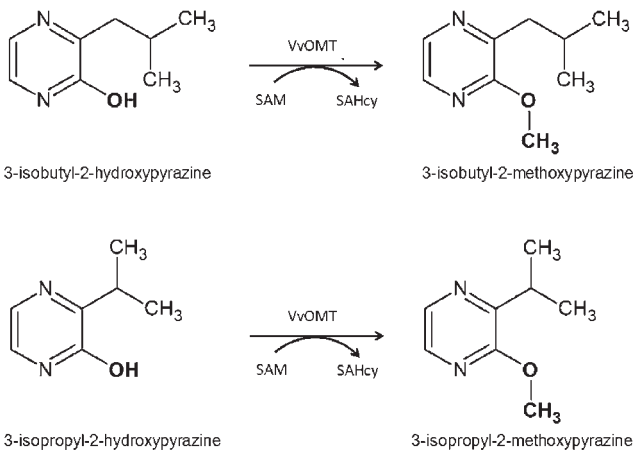


**Figure 1.** Proposed biosynthesis pathway for 3-alkyl-2-methoxypyrazine. The reaction implies that the methylation of 3-alkyl-2-hydroxypyrazine is mediated by a *Vitis vinifera* *O*-methyltransferase protein (VvOMT) in the presence of *S*-adenosyl-L-methionine (SAM) as a methyl group donor. As a product of this reaction, 3-alkyl-2-methoxypyrazine and *S*-adenosylhomocysteine are generated (based on Hashizume et al. 2001[13]).

production cycle have been described. However, there is little information on MPs biosynthesis. Some studies suggest that the pathway for 3-alkyl-2-methoxypyrazine biosynthesis begins with an amino acid such as valine and leucine,[2,23−26] but the remainder of the biosynthetic pathway is not yet described. According to Hashizume et al.,[13] the final step in the biosynthesis of 3-alkyl-2-methoxypyrazines involves the methylation of 3-alkyl-2-hydroxypyrazines, which is mediated by an *O*-methyltransferase (OMT) in the presence of *S*-adenosyl-L-methionine (SAM) as the methyl group donor (Figure 1).

A SAM-dependent OMT enzyme capable of methylating hydroxypyrazines has been detected in crude extracts from grapevine tissues[13] and subsequently purified, characterized and sequenced, that is, the N-terminal partial sequence.[27] These data allowed the detection and characterization of two *Vitis vinifera* *O*-methyltransferase genes (*VvOMT1* and *VvOMT2*) with the ability to methylate hydroxypyrazines,[16] but there is no evidence at atomic level that can explain the differences in the kinetic activities observed. This study provides evidence to understand why VvOMT1 and VvOMT2 proteins show different activities in the final step of MPs biosynthesis. This information could be useful for future agricultural applications in order to modulate MPs concentrations in grapevines.

## MATERIALS AND METHODS

**Grape Samples.** Grapevine samples were collected from commercial Carmenere vineyards during the 2008−2009 growing season in Colchagua Valley, Chile, 34°30′ S, longitude 70°53′ W. Cluster samples were frozen in liquid nitrogen and stored at −80 °C until used.

**Isolation of *VvOMT1* and *VvOMT2*.** Total RNA was isolated from frozen berries using protocol described by Reid *el al.*[28] RNA was precipitated by adding 0.30 vol of 8 M LiCl and stored at 4 °C overnight. The pellet was suspended in 170 μL DEPC-treated $H_2O$. The eluent was cleaned using a spin column, RNA dilution buffer and RNA wash buffer from the SV Total RNA Isolation System (Promega), and resuspended in 100 μL DEPC-treated $H_2O$. Genomic DNA was removed from 50 μL aliquots of total RNA preparations of each sample by digestion with RNase-free DNase I (Ambion) according to the manufacturer's protocol. cDNAs were synthesized from 1 μg of total RNA using the Revertaid First Strand cDNA Synthesis K1622 Kit (Fermentas) using an oligo$(dT)_{18}$ primer according to the manufacturer's instructions. *VvOMT* sequences were amplified by PCR techniques using the same primers described by Dunlevy et al.[16] PCR products were cloned into a pGemT Easy Vector (Promega) and sequenced (Macrogen, Korea, External service).

**Homology Modeling.** The reference structure used to build the homology model was the isoflavone *O*-methyltransferase (IOMT) of *Medicago sativa* (ID code: 1FP2; resolution: 1.4 Å; R-Value: 0.217), which was obtained from the protein data bank (Research Collaboratory for Structural Bioinformatics, RCSB, http://www.rcsb.org/pdb). IOMT and *Vitis vinifera* OMTs (VvOMT1 and VvOMT2) sequences were aligned using Clustal W.[29] Using this alignment and the software MODELLER version 9v6,[30] homology models were built for both proteins.

**Docking Simulations.** AutoDock 4[31] was used to explore the binding pocket of the IBHP and IPHP substrates in the active sites of the VvOMT1 and VvOMT2 proteins. Density functional theory (DFT) methods[32] were used that considered B3LYP [33,34] and the 3-21 g* basis set. MAESTRO[35] graphical interface and OPLS[36] force field were used to assign partial charges for the VvOMT1:SAM and VvOMT2:SAM complexes. Autodock Tools (ADT) was used to prepare both complexes and the ligand. The grid size used was 50 × 50 × 50 point with a spacing of 0.375 Å, which includes all the key residues of the active site. Visual inspections of the results were performed using the MGL Tools package.[37]

**QM/MM Approach.** Quantum mechanics/molecular mechanics (QM/MM) calculations were performed using the QSite software[38] of Schrödinger's 2008 suite, which combines the Jaguar[39] and Impact [40,41] codes. Jaguar was used for the QM region and impact molecular modeling code for the MM region.

In order to evaluate enthalpy affinity, interaction energies were calculated using the following equation:

$$E_{\text{interaction}} = E_{\text{complex(VvOMT:SAM:IBHP/IPHP)}} - (E_{\text{VvOMT:SAM}} + E_{\text{IBHP/IPHP}})$$

## RESULTS AND DISCUSSION

**VvOMT Proteins.** The pathway for 3-alkyl-2-methoxypyrazines (MPs) biosynthesis in plants is still relatively unclear. Some alternatives have been proposed, but none have been proven.[2,23−26] In previous work a *S*-adenosyl-L-methionine (SAM)-dependent *O*-methyltransferase (OMT) enzyme was purified from cv. Cabernet Sauvignon and described to be capable of methylating 3-alkyl-2-hydroxypyrazines (HPs).[27] Additionally, Dunlevy et al.[16] isolated the full-length sequences of two grape OMT genes (*VvOMT1* and *VvOMT2*) from cv. Cabernet Sauvignon and demonstrated that both were able to methylate HPs to produce MPs. VvOMT1 had higher catalytic activity against IBHP compared to IPHP, whereas no differences were observed for VvOMT2. However, kinetic parameters of each recombinant protein using IBHP and IPHP as substrates showed that VvOMT1 had a similar substrate preference with similar $K_m$ values and higher turnover number for IBHP compared to IPHP. On the

```
VvOMT1          1   MVSRSEIDDVLKISREADEAELMLQGQANIWRHMFAFADSMALKCAVELRIADI
VvOMT2          1   MVGTSENGDVLKVSSEADETELMLQGQANIWRHMFAFADSMALKCAVELRIADI
IOMT            1   ----------MASSINGRKPSEIFKAQALLYKHIYAFIDSMSLKWAVEMNIPNI

VvOMT1         55   IHSQARPITLSQIATCIDSPSPDITCLARIMRFLVRAKIFTAAPPPQSDGGETL
VvOMT2         55   IHSHARPITLSQIATCIDSPSPDITCLARIMRFLVRAKIFTAAPPPQSDGGETL
IOMT           45   IQNHGKPISLSNLVSILQVPSSKIGNVRRLMRYLAHNGFFEIITKEEES-----

VvOMT1        109   YGLTPSSKWLLHDADLSLAPMVLMENHPFLMAPWHCFGTCVKEGGIA-FEKAHG
VvOMT2        109   YGLTPSSKWLLHDAELSLAPMVLMENHPSLMAPWHCFGTCVKEGGIA-FEKAHG
IOMT           94   YALTVASELLVRGSDLCLAPMVECVLDPTLSGSYHELKKWIYEEDLTLFGVTLG
                                        S

VvOMT1        162   RQIWDFASENPEFNKLFNDGMACTAKVVMGEVVAAYKDGFGSIRTLVDVGGGTG
VvOMT2        162   HQIWDLASEKPEFNKLFNDGMACTAKISIKAVIAAYKDGFGSIGTLVDVGGGTG
IOMT          148   SGFWDFLDKNPEYNTSFNDAMASDSKL-INLALRDCDFVFDGLESIVDVGGGTG
                          S   S                                S S

VvOMT1        216   GAVAEVVKAYPHIKGINFDLPHVVASAPAYEGVSHVGGDMFESIPNADAIFMKW
VvOMT2        216   GAVAEVVKAYPHIKGINFDLPHVVATAPAYKGVSHVGGDMFESIPDADAIFMKW
IOMT          201   TTAKIICETFPKLKCIVFDRPQVVENLSGSNNLTYVGGDMFTSIPNADAVLLKY
                              SS                        SS           S

VvOMT1        270   IMHDWSDEDCIKILKNCRKAVPE--KTGKIIIVDGVI-REDSDDPFDKTRLVFD
VvOMT2        270   ILHDWNDEDCVKILKNCRKAIPE--KTGKVIIVDGVI-REDGYEPFDETRLVLD
IOMT          255   ILHNWTDKDCLRILKKCKEAVTNDGKRGKVTIIDMVIDKKKDENQVTQIKLLMD
                      C S                          C              S

VvOMT1        321   LLMMAHSSNGKERSEVEWKKVLEEGGFPRYRIMEISISTLPMIIEAYP
VvOMT2        321   LVMMAHSSHGQERTEVEWKKLLEEGGFPRYRILKIP--TLQMIIEAYP
IOMT          309   VNMACL--NGKERNEEEWKKLFIEAGFQHYKIS--PLTGFLSLIEIYP
                     SS        C
```

| | VvOMT1 | VvOMT2 |
|---|---|---|
| IOMT | 38% (identity)<br>68% (similarity) | 37% (identity)<br>68% (similarity) |
| VvOMT1 | - | 87% (identity)<br>96% (similarity) |

**C** Catalytic residue

**S** Substrate binding

**Figure 2.** Amino acid alignment, identity and similarity percentages for two *Vitis vinifera* *O*-methyltransferases (VvOMT1, XP_002277602.1 and VvOMT2, XP_002277476.1) with *Medicago sativa* isoflavone *O*-methyltransferase (IOMT, AF023481) used as the reference structure for building the homology models.

other hand, VvOMT2 had higher affinity for IBHP than IPHP but conversely had a lower turnover number against IBHP than IPHP.[16] Furthermore, MPs accumulation in skin and flesh of cv. Cabernet Sauvignon grapes berries was associated with higher VvOMT1 gene expression in these tissues while high levels of MPs in roots was correlated with VvOMT2 gene expression.[16]

It is well-known that the main methoxypyrazine red wine problem is related to IBMP,[1,7,8,15,17−19] which has been reported in very high levels in Carmenere wines.[9] Functional information of VvOMT1 and VvOMT2 from cv. Cabernet Sauvignon has been solved.[16,27] However, there are no structural reports and the molecular features responsible for the substrate-requirement of these isoforms are unknown. In this paper, *VvOMT1* and *VvOMT2* were isolated from cv. Carmenere and VvOMT1:SAM:IBHP/IPHP and VvOMT2:SAM:IBHP/IPHP complexes compared at the atomic level, identifying the crucial amino acid residues responsible for the interaction during the methylation of HP substrates, precursor of MPs.[16,27]

VvOMT1 encodes a protein of 368 amino acids, and VvOMT2 encodes a 366 amino acid protein. These proteins have 87% identity (96% similarity) to each other and 38% and 37% identity (68% similarity) respectively, to the *Medicago sativa* isoflavone *O*-methyltransferase (IOMT) (Figure 2), a protein with a characterized crystal structure.[42] Some differences were observed in residues near the active site of the protein, which have implications for protein−substrate affinity. The main differences in the equivalent residues in the active site were F319−L322 for VvOMT1 and L319−V322 for VvOMT2, respectively (Figure 2). It was interesting to address whether there was a possibility of gene mutation when comparing *VvOMT1* and *VvOMT2* from cv. Carmenere and cv. Cabernet Sauvignon that could explain the differences in MPs concentrations.[9] After alignment analyses of sequenced clones, no differences were observed (data not shown).

VvOMT1 and VvOMT2 correspond to members of the class II *O*-methyltransferase family in plants.[16] This family of enzymes is dependent on *S*-adenosyl-L-methionine (SAM) as the methyl group donor. IOMT has a tertiary structure consisting of a large C-terminal catalytic domain responsible for SAM binding and substrate methylation with a small N-terminal domain involved in dimerization and formation of the back wall of the substrate binding site.[42] Active site regions of VvOMT1 and VvOMT2 correspond to conserved sites in key catalytic residues of OMT proteins.[42]

**Molecular Simulations.** During docking simulations, AutoDock was used to explore the binding pockets of both VvOMT proteins with IBHP and IPHP substrates. AutoDock uses a grid-based method for energy evaluation providing high quality predictions for ligand conformations, binding energies and good correlations between predicted inhibition constants and experimental ones (http://autodock.scripps.edu/). IBHP and IPHP were poorly described in the force field used for these simulations.

**Table 1. Residues Observed in the Active Site of VvOMT1: SAM:IBHP/IPHP and VvOMT2:SAM:IBHP/IPHP Complexes at Different Visual Openings in the QM/MM Grid**

| complex | residues 2 Å from substrate | additional residues 2.5 Å from substrate | additional residues 3 Å from substrate |
|---|---|---|---|
| VvHPMT1:SAM:IBHP | H272 | M129 | M132 |
| | | F319 | M182 |
| | | L322 | H326 |
| | | M323 | |
| VvHPMT2:SAM:IBHP | W269 | H272 | M129 |
| | T185 | L319 | M132 |
| | | | M182 |
| | | | C184 |
| | | | L358 |
| VvHPMT1:SAM:IPHP | H272 | M129 | H135 |
| | | M132 | M182 |
| | | F319 | F178 |
| | | L322 | M323 |
| | | | H326 |
| VvHPMT2:SAM:IPHP | T185 | C184 | M129 |
| | | W269 | M182 |
| | | L319 | |
| | | L358 | |

Therefore, and to improve electronic and structural property characterizations of IBHP and IPHP (ligands), density functional theory (DFT) methods[32] were used, which considered B3LYP[33,34] and the 3-21 g* basis set. MAESTRO[35] graphical interface and OPLS[36] force field were used to assign partial charges for the VvOMT1:SAM and VvOMT2:SAM complexes. Autodock Tools (ADT) was used to prepare both complexes and the ligands. The grid size used was 50 × 50 × 50 point with a spacing of 0.375 Å, which included all the key residues of the active site. Visual inspections of the results were done using the MGL Tools package.[37]

The homology models built for VvOMT1 and VvOMT2 showed good accuracy and stereochemical quality (Procheck and Prosa analysis, data not shown). In order to explore the pocket binding of the VvOMTs, docking simulations were performed using IBHP and IPHP as a substrates against the active site of the enzyme:SAM systems. The lowest energy and cluster obtained showed mainly hydrophobic interactions between substrates and the amino acids that formed the active site.

Gradual increases in the field of vision around the substrate showed differences in the number and type of residues around IBHP and IPHP (Table 1). In the 2 Å field of view for the IBHP substrate, just one catalytic residue (H272) was observed in the VvOMT1:SAM:IBHP complex. For the VvOMT2:SAM:IBHP complex, this residue only appears over 2.5 Å. At this distance, two new residues (F319, L322) related to SAM binding were only observed in the VvOMT1:SAM:IBHP complex. The equivalent residues in the second complex (VvOMT2:SAM:IBHP) were L319 and V322. L319 was visible at 2.5 Å, whereas V322 only appeared over 5 Å in IBHP. As illustrated in Table 1, over 3 Å both complexes share the same substrate binding residues (M132, M182).

When observing the visual results using IPHP as a substrate, in the 2 Å field of view for this substrate, just one catalytic residue (H272) was observed in the VvOMT1:SAM:IPHP complex, the same way as shown for the IBHP substrate. At 2.5 Å for IPHP, two residues (L319, V322) related with SAM binding were observed in the VvOMT1:SAM:IPHP complex, but not in the second complex (VvOMT2:SAM:IPHP). At 3 Å both complexes share just two residues (M129, M182). Thus, these spatial conformation differences observed in VvOMTs:SAM complexes using IBHP and IPHP as substrates, create differences in the clustering of active site residues that distinguish these proteins. This has implications in hydrophobicity, positioning and spatial relationships.

In order to refine the structure obtained in the docking simulations, QM/MM calculations were performed. Due to the fact that interactions between ligands and proteins are no covalent, ligands (IBHP, IPHP substrates and SAM) were defined as the QM region and the protein as the MM region. The QM region was studied using density functional theory (DFT) methods, B3LYP and the 6-31++G(d,p) basis set. The MM region was studied using the OPLS-AA molecular mechanics force field.[43,44]

The results indicated several hydrophobic interactions existed between substrates and the binding pockets of VvOMT1 and VvOMT2. Figure 3 shows the active site of the VvOMT1/2: SAM:IBHP/IPHP complexes, and the spatial arrangement adopting H272 and M182 with SAM and substrates as a part of these complexes can be observed. In VvOMT1:SAM:IBHP/IPHP, the layout acquired by IBHP and IPHP were favorable for achieving the transition state necessary for the transfer of the methyl group from the donor (SAM) to the receptor (IBHP, IPHP). An important hydrogen bond between $N_{IBHP}$- - -H-$N_{IMIDAZOLE}$ of the H272 residue, which had a distance of 1.9 Å for both complexes (VvOMT1:SAM:IBHP/IPHP), was also observed (Figure 3a and b). Previous reports have shown that H272 is a catalytic residue in SAM-dependent *O*-methyltransferase enzymes.[42] The distance between the IBHP and IPHP oxygen atom (receptor) and carbon atom of the methyl group of the SAM (donor) were 6.3 Å and 6.6 Å respectively. Between them, it was possible to observe the M182 residue interacting with SAM and IBHP and IPHP substrates.

Figure 3c and d shows the active site formed in the VvOMT2: SAM:IBHP/IPHP complexes. In this interaction, both substrates (IBHP, IPHP) acquired an unfavorable layout to attain the transition state necessary for transfer of the methyl group. It was possible to measure the distances between these molecules (Figure 3c and d). Therefore, the distance between the IBHP/IPHP substrate nitrogen atom and the hydrogen atom of the $N_{IMIDAZOLE}$ group of H272 were 7.4 Å and 7 Å, and the distance between the IBHP/IPHP oxygen atom and the carbon atom of the SAM methyl group were 7.2 Å and 7.8 Å, respectively.

Dunlevy et al.[16] showed VvOMT1 has greater catalytic activity toward IBHP than VvOMT2. Therefore, it is possible to see differences in $k_{cat}/K_m$ such as $108.7 \times 10^{-3}$ ($M^{-1}s^{-1}$) for VvOMT1 and $11.9 \times 10^{-3}$ ($M^{-1}s^{-1}$) for VvOMT2. During this methylation, the recombinant VvOMTs showed specific activity values of 1.4 (pkat $mg^{-1}$) for VvOMT1 and 0.2 (pkat $mg^{-1}$) for VvOMT2.[16]

The evidence presented here explains previously reported[16] kinetic differences between VvOMT1/2 through an atomic level

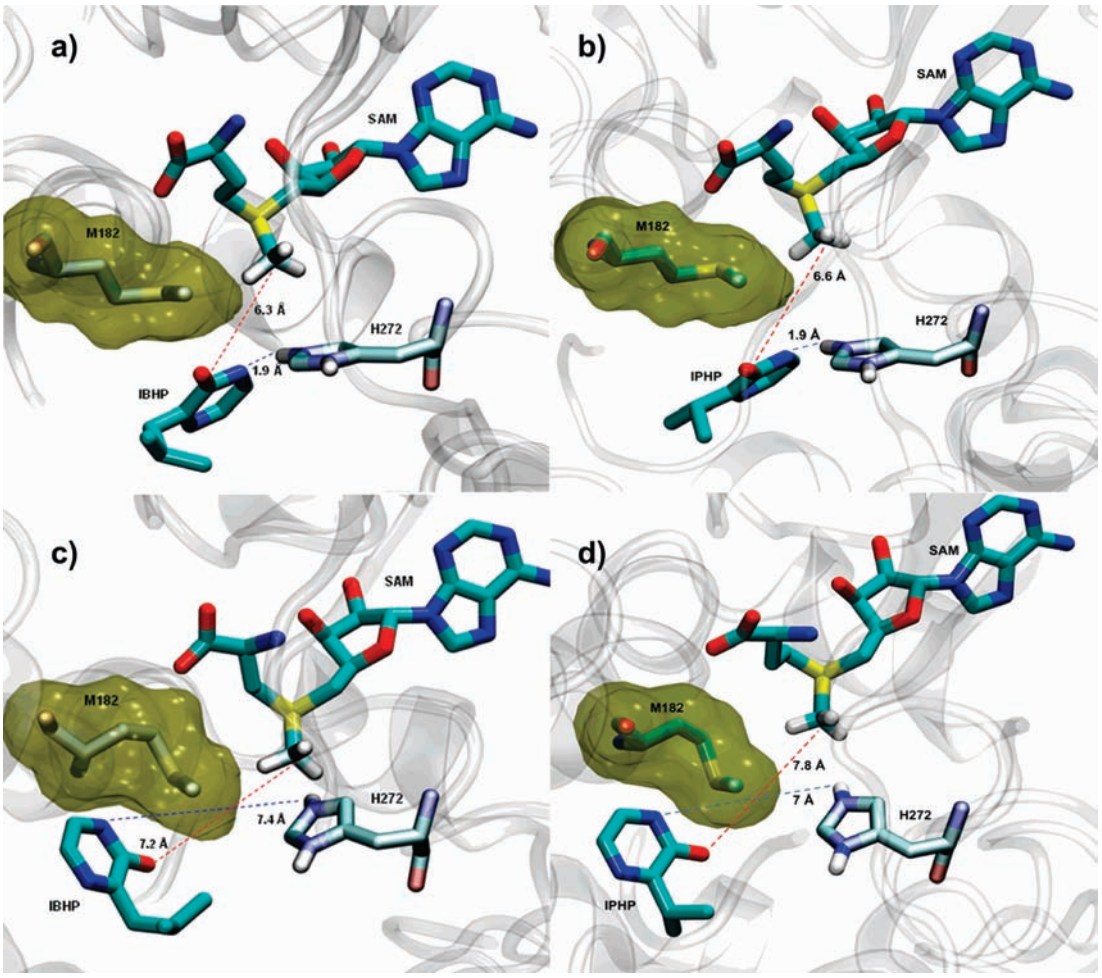


**Figure 3.** Representation view of the VvOMT1:SAM:IBHP/IPHP and VvOMT2:SAM:IBHP/IPHP complexes obtained through QM/MM calculations. The residue in surface representation corresponds to M182, which correspond to a substrate-binding residue. For a and b, the hydrogen bond interaction between the nitrogen atom of hydroxypyrazine (IBHP/IPHP) and the hydrogen of the imidazole group of H272 amino acid are visualized. (a) Representation view of VvOMT1:SAM:IBHP complex. The distance between the oxygen atom of IBHP and the carbon atom of the SAM methyl group is 6.3 Å. (b) Representation view of VvOMT1:SAM:IPHP complex. The distance between the oxygen atom of IPHP and the carbon atom of the SAM methyl group is 6.6 Å. (c) Representation view of the VvOMT2:SAM:IBHP complex. The distance between the nitrogen atom IBHP and the hydrogen atom of the H272 imidazole group is 7.4 Å. The distance between the IBHP oxygen atom and the carbon atom of the SAM methyl group is 7.2 Å. (d) Representation view of the VvOMT2:SAM:IPHP complex. The distance between the nitrogen atom ofIPHP and the hydrogen atom of the H272 imidazole group is 7 Å. The distance between the IPHP oxygen atom and the carbon atom of the SAM methyl group is 7.8 Å.

vision on how IBHP and IPHP substrates interact with these proteins and SAM. High correlation ($r^2$ = 0.92) between affinity enthalpy (Table 2) and experimental data[16] show that the entropic contribution in this interaction is low, allowing a direct correlation between enthalpy and affinity free energy to be established.

VvOMT1 shows a more favorable enthalpy affinity for IBHP than IPHP during MP production. This could be explained by differences in the number of aliphatic carbons between IBHP (4 carbons) and IPHP (3 carbons) resulting in greater hydrophobicity for IBHP. Furthermore, in order to produce the catalytic reaction a hydrogen bonds network between substrate and the catalytic residue H272 is required. This interaction promotes methyl group transfer from SAM to substrate in order to produce MP.

VvOMT2 shows a mutation in two important residues (L319, V322) in the microenvironment of the active site. These mutations produce a less hydrophobic cavity in VvOMT2 than in VvOMT1. Under these conditions, substrate aliphatic chains generate interactions on a cavity that is located beyond of the H272 residue, hampering the generation of hydrogen bonds with this catalytic residue and decreasing the probability that the substrates acquire the conformation required for generating the transition state.

**Table 2. Theoretical Results for Enzymatic Activities in VvOMT1:SAM:IBHP/IPHP and VvOMT2:SAM:IBHP/IPHP Complexes**

| protein | substrate | enthalpy energy QM/MM (kcal mol$^{-1}$) |
|---|---|---|
| VvOMT1 | IBHP (108.7[a]) | −151.6 |
| | IPHP (65.7[a]) | −134.3 |
| VvOMT2 | IBHP (11.9[a]) | −56.7 |
| | IPHP (13.9[a]) | −77.2 |

[a] Kcat/Km × $10^{-3}$ ($M^{-1}$ $s^{-1}$) extracted from Dunlevy et al. (2010)[16].

In all complexes, the distances between the substrate oxygen atom and the carbon atom of the SAM methyl group showed no significant differences and thus it is not possible to ascribe to it differences in the observed catalytic activity.[16] Furthermore, evidence suggests that the main structural difference between VvOMT1 and VvOMT2 is related to the fact that the substrate affinity site is closer to the M182 residue in VvOMT2, forming a steric impediment between substrate and SAM, limiting the formation of the transition state for methyl transfer (Figure 3c, 3d).

Both genes (*VvOMT1* and *VvOMT2*) encode proteins capable of methylating HPs to produce MPs. However, VvOMT1 appears to be more important in the biosynthesis of this compound in grapevines. Therefore, M182 and H272 could be very important residues to be manipulated in order to modulate MPs levels in grapevines.

## AUTHOR INFORMATION

### Corresponding Author

*E-mail: ymoreno@utalca.cl.

### Author Contributions

⊥J.V. and X.L. contributed equally to this work.

## ACKNOWLEDGMENT

We thank Viña Casa Silva Chile for providing wine grapes for this investigation. We acknowledge Consorcio del Vino Tecnovid S.A., CONICYT grant AT24091085 and Programa Bicentenario de Ciencia y Tecnologia, ACT/24 (F. G-N) for their financial support. We thank Dr. AlejandoYevenes for critical discussion of this work.

## REFERENCES

(1) de Boubee, D. R.; Van Leeuwen, C.; Dubourdieu, D. Organoleptic impact of 2-methoxy-3-isobutylpyrazine on red Bordeaux and Loire wines. Effect of environmental conditions on concentrations in grapes during ripening. *J. Agric. Food Chem.* **2000**, *48*, 4830–4834.

(2) Murray, K. E.; Whitfield, F. B. The occurrence of 3-alkyl-2-methoxypyrazines in raw vegetables. *J. Sci. Food Agric.* **1975**, *26*, 973–986.

(3) Mazida, M. M.; Salleh, M. M.; Osman, H. Analysis of volatile aroma compounds of fresh chilli (*Capsicum annuum*) during stages of maturity using solid phase microextraction (SPME). *J. Food Compos. Anal.* **2005**, *18*, 427–437.

(4) Neta, E. R. D.; Miracle, R. E.; Sanders, T. H.; Drake, M. A. Characterization of alkylmethoxypyrazines contributing to earthy/bell pepper flavor in farmstead cheddar cheese. *J. Food Sci.* **2008**, *73*, C632–C638.

(5) Lasekan, O.; Buettner, A.; Christlbauer, M. Investigation of important odorants of palm wine (*Elaeis guineensis*). *Food Chem.* **2007**, *105*, 15–23.

(6) Bayonove, C.; Cordinnier, R.; Dubois, P. Etude d'une fraction caractéristique de l'arôme du raisin de la variété Cabernet Sauvignon; mise en évidence de la 2-méthoxy-3-isobutylpyrazine. *CR. Acad. Sci. Paris* **1975**, *281*, 75–78.

(7) de Boubee, D. R.; Cumsille, A. M.; Pons, M.; Dubourdieu, D. Location of 2-methoxy-3-isobutylpyrazine in Cabernet Sauvignon grape bunches and its extractability during vinification. *Am. J. Enol. Vitic.* **2002**, *53*, 1–5.

(8) Hashizume, K.; Umeda, N. Methoxypyrazine content of Japanese red wines. *Biosci. Biotechnol. Biochem.* **1996**, *60*, 802–805.

(9) Belancic, A.; Agosin, E. Methoxypyrazines in grapes and wines of *Vitis vinifera* cv. Carmenere. *Am. J. Enol. Vitic.* **2007**, *58*, 462–469.

(10) Allen, M. S.; Lacey, M. J.; Harris, R. L. N.; Brown, W. V. Contribution of methoxypyrazines to Sauvignon blanc wine aroma. *Am. J. Enol. Vitic.* **1991**, *42*, 109–112.

(11) Hashizume, K.; Samuta, T. Grape maturity and light exposure affect berry methoxypyrazine concentration. *Am. J. Enol. Vitic.* **1999**, *50*, 194–198.

(12) Sala, C.; Busto, O.; Guasch, J.; Zamora, F. Influence of vine training and sunlight exposure on the 3-alkyl-2-methoxypyrazines content in musts and wines from the *Vitis vinifera* variety cabernet sauvignon. *J. Agric. Food Chem.* **2004**, *52*, 3492–3497.

(13) Hashizume, K.; Tozawa, K.; Endo, M.; Aramaki, I. *S*-adenosyl-L-methionine-dependent *O*-methylation of 2-hydroxy-3-alkylpyrazine in wine grapes: A putative final step of methoxypyrazine biosynthesis. *Biosci. Biotechnol. Biochem.* **2001**, *65*, 795–801.

(14) Lacey, M. J.; Allen, M. S.; Harris, R. L. N.; Brown, W. V. Methoxypyrazines in Sauvignon blanc grapes and wines. *Am. J. Enol. Vitic.* **1991**, *42*, 103–108.

(15) Ryona, I.; Pan, B. S.; Intrigliolo, D. S.; Lakso, A. N.; Sacks, G. L. Effects of cluster light exposure on 3-isobutyl-2-methoxypyrazine accumulation and degradation patterns in red wine grapes (*Vitis vinifera* L. cv. Cabernet franc). *J. Agric. Food Chem.* **2008**, *56*, 10838–10846.

(16) Dunlevy, J. D.; Soole, K. L.; Perkins, M. V.; Dennis, E. G.; Keyzers, R. A.; Kalua, C. M.; Boss, P. K. Two *O*-methyltransferases involved in the biosynthesis of methoxypyrazines: Grape-derived aroma compounds important to wine flavour. *Plant Mol. Biol.* **2010**, *74*, 77–89.

(17) Chapman, D. M.; Thorngate, J. H.; Matthews, M. A.; Guinard, J. X.; Ebeler, S. E. Yield effects on 2-methoxy-3-isobutylpyrazine concentration in Cabernet Sauvignon using a solid phase microextraction gas chromatography/mass spectrometry method. *J. Agric. Food Chem.* **2004**, *52*, 5431–5435.

(18) Sala, C.; Busto, O.; Guasch, J.; Zamora, F. Contents of 3-alkyl-2-meithoxypyrazines in musts and wines from *Vitis vinifera* variety Cabernet Sauvignon: influence of irrigation and plantation density. *J. Sci. Food Agric.* **2005**, *85*, 1131–1136.

(19) Kotseridis, Y.; Anocibar-Beloqui, A.; Bayonove, C.; Baumes, R.; Bertrand, A. Effects of selected viticultural and enological factors on levels of 2-methoxy-3-isobutylpyrazine in wines. *J. Int. Sci. Vigne Vin.* **1999**, *33*, 19–23.

(20) Hashizume, K.; Samuta, T. Green odorants of grape cluster stem and their ability to cause a wine stemmy flavor. *J. Agric. Food Chem.* **1997**, *45*, 1333–1337.

(21) Pickering, G. J.; Spink, M.; Kotseridis, Y.; Inglis, D.; Brindle, I. D.; Sears, M.; Beh, A. L. Yeast strain affects 3-isopropyl-2-methoxypyrazine concentration and sensory profile in Cabernet Sauvignon wine. *Aust. J. Grape Wine Res.* **2008**, *14*, 230–237.

(22) Pickering, G. J.; Lin, Y.; Reynolds, A.; Soleas, G.; Riesen, R.; Brindle, I. The influence of *Harmonia axyridis* on wine composition and aging. *J. Food Sci.* **2005**, *70*, S128–S135.

(23) Cheng, T. B.; Reineccius, G. A.; Bjorklund, J. A.; Leete, E. Biosynthesis of 2-methoxy-3-isopropilpyrazine in *Pseudomonas perolens*. *J. Agric. Food Chem.* **1991**, *39*, 1009–1012.

(24) Seifert, R. M.; Buttery, R. G.; Guadagni, D. G.; Black, D. R.; Harris, J. G. Synthesis of some 2-methoxy-3-alkylpyrazines with strong bell pepper-like odors. *J. Agric. Food Chem.* **1970**, *18*, 246–249.

(25) Gallois, A.; Kergomard, A.; Adda, J. Study of the biosynthesis of 3-isopropyl-2-methoxypyrazine produced by *Pseudomonas taetrolens*. *Food Chem.* **1988**, *28*, 299–309.

(26) Jones, R. G. Pyrazines and related compounds. I. A new synthesis of hydroxypyrazines. *J. Am. Chem. Soc.* **1949**, *71*, 78–81.

(27) Hashizume, K.; Tozawa, K.; Hiraga, Y.; Aramaki, I. Purification and characterization of a *O*-methyltransferase capable of methylating 2-hydroxy-3-alkylpyrazine from *Vitis vinifera* L. (cv. Cabernet Sauvignon). *Biosci. Biotechnol. Biochem.* **2001**, *65*, 2213–2219.

(28) Reid, K. E.; Olsson, N.; Schlosser, J.; Peng, F.; Lund, S. T. An optimized grapevine RNA isolation procedure and statistical determination of reference genes for real-time RT-PCR during berry development. *BMC Plant Biol.* **2006**, *14* (6), 27.

(29) Thompson, J. D.; Higgins, D. G.; Gibson, T. J. Clustal-W - Improving the sensitivity of progressive multiple sequence alignment through sequence weighting, position-specific gap penalties and weight matrix choice. *Nucleic Acids Res.* **1994**, *22*, 4673–4680.

(30) Sali, A.; Blundell, T. L. Comparative protein modelling by satisfaction of spatial restraints. *J. Mol. Biol.* **1993**, *234*, 779–815.

(31) Morris, G. M.; Goodsell, D. S.; Halliday, R. S.; Huey, R.; Hart, W. E.; Belew, R. K.; Olson, A. J. Automated docking using a Lamarckian genetic algorithm and an empirical binding free energy function. *J. Comput. Chem.* **1998**, *19*, 1639–1662.

(32) Andzelm, J.; Wimmer, E. Density functional gaussian-type-orbital approach to molecular geometries, vibrations, and reaction energies. *J. Chem. Phys.* **1992**, *96*, 1280–1303.

(33) Becke, A. D. Density-functional thermochemistry 0.5. Systematic optimization of exchange-correlation functionals. *J. Chem. Phys.* **1997**, *107*, 8554–8560.

(34) Lee, C. T.; Yang, W. T.; Parr, R. G. Development of the Colle-Salvetti correlation-energy formula into a functional of the electron-density. *Phys. Rev. B.* **1988**, *37*, 785–789.

(35) Maestro 8.5.207; Schrödinger, I. S. F. A., : Suite 1180, Portland, OR.

(36) Dauberosguthorpe, P.; Roberts, V. A.; Osguthorpe, D. J.; Wolff, J.; Genest, M.; Hagler, A. T. Structure and energetics of ligand-binding to proteins - Escherichia-coli dihydrofolate reductase trimethoprim, a drug-receptor system. *Proteins* **1988**, *4*, 31–47.

(37) Sanner, M. F. Python: A programming language for software integration and development. *J. Mol. Graph.* **1999**, *17*, 57–61.

(38) QSite v. 5.0, S., Inc., LLC: New York, NY. 2008.

(39) Jaguar 5.5, S., Inc.: Portland, OR. 1991−2003.

(40) IMPACT 2.7, S., Inc.: Portland, OR. 2003.

(41) Banks, J. L.; Beard, H. S.; Cao, Y. X.; Cho, A. E.; Damm, W.; Farid, R.; Felts, A. K.; Halgren, T. A.; Mainz, D. T.; Maple, J. R.; Murphy, R.; Philipp, D. M.; Repasky, M. P.; Zhang, L. Y.; Berne, B. J.; Friesner, R. A.; Gallicchio, E.; Levy, R. M. Integrated modeling program, applied chemical theory (IMPACT). *J. Comput. Chem.* **2005**, *26*, 1752–1780.

(42) Zubieta, C.; He, X. Z.; Dixon, R. A.; Noel, J. P. Structures of two natural product methyltransferases reveal the basis for substrate specificity in plant *O*-methyltransferases. *Nat. Struct. Biol.* **2001**, *8*, 271–279.

(43) Jorgensen, W. L.; Maxwell, D. S.; TiradoRives, J. Development and testing of the OPLS all-atom force field on conformational energetics and properties of organic liquids. *J. Am. Chem. Soc.* **1996**, *118*, 11225–11236.

(44) Kaminski, G. A.; Friesner, R. A.; Tirado-Rives, J.; Jorgensen, W. L. Evaluation and reparametrization of the OPLS-AA force field for proteins via comparison with accurate quantum chemical calculations on peptides. *J. Phys. Chem. B* . **2001**, *105*, 6474–6487.